Contributions of cellular leak pathways to net NaHCO3 and NaCl absorption.

P A Preisig, R J Alpern

J Clin Invest. 1989;83(6):1859-1867. https://doi.org/10.1172/JCI114092.

Research Article

Proton and formic acid permeabilities were measured in the in vivo microperfused rat proximal convoluted tubule by examining the effect on intracellular pH when [H] and/or [formic acid] were rapidly changed in the luminal or peritubular fluids. Apical and basolateral membrane H permeabilities were 0.52 +/- 0.07 and 0.67 +/- 0.18 cm/s, respectively. Using these permeabilities we calculate that proton backleak from the luminal fluid to cell does not contribute significantly to net proton secretion in the early proximal tubule, but may contribute in the late proximal tubule. Apical and basolateral membrane formic acid permeabilities measured at extracellular pH 6.62 were 4.6 +/- 0.5 X 10(-2) and 6.8 +/- 1.5 X 10(-2) cm/s, respectively. Control studies demonstrated that the formic acid permeabilities were not underestimated by either the simultaneous movement of formate into the cell or the efflux of formic acid across the opposite membrane. The measured apical membrane formic acid permeability is too small to support all of transcellular NaCl absorption in the rat by a mechanism that involves Na/H-Cl/formate transporters operating in parallel with formic acid nonionic diffusion.

Contributions of Cellular Leak Pathways to Net $NaHCO_3$ and NaCl Absorption

Patricia A. Preisig and Robert J. Alpern
Department of Internal Medicine, The University of Texas Southwestern Medical Center, Dallas, Texas 75235-9030

Abstract

Proton and formic acid permeabilities were measured in the in vivo microperfused rat proximal convoluted tubule by examining the effect on intracellular pH when [H] and/or [formic acid] were rapidly changed in the luminal or peritubular fluids. Apical and basolateral membrane H permeabilities were 0.52±0.07 and 0.67±0.18 cm/s, respectively. Using these permeabilities we calculate that proton backleak from the luminal fluid to cell does not contribute significantly to net proton secretion in the early proximal tubule, but may contribute in the late proximal tubule. Apical and basolateral membrane formic acid permeabilities measured at extracellular pH 6.62 were $4.6\pm0.5 \times 10^{-2}$ and $6.8\pm1.5 \times 10^{-2}$ cm/s, respectively. Control studies demonstrated that the formic acid permeabilities were not underestimated by either the simultaneous movement of formate into the cell or the efflux of formic acid across the opposite membrane. The measured apical membrane formic acid permeability is too small to support all of transcellular NaCl absorption in the rat by a mechanism that involves Na/H-Cl/formate transporters operating in parallel with formic acid nonionic diffusion.

Introduction

Transepithelial bicarbonate absorption in the proximal convoluted tubule (PCT)[1] involves apical membrane H secretion that is mediated by an Na/H antiporter and probably an H-translocating ATPase (1). Base generated within the cell exits across the basolateral membrane via the $Na(HCO_3)_3$ symporter (1). Across both membranes the electrochemical driving force for passive H movement is from either the luminal or peritubular fluid into the cell. The backleak of H from lumen to cell across the apical membrane is counterproductive to HCO_3 absorption. Conversely, the leak of H across the basolateral membrane from peritubular fluid to cell is equivalent to base efflux, and thus supports transepithelial HCO_3 absorption.

30–60% of NaCl absorption in the late proximal tubule has been shown to be electroneutral and transcellular (2–6). Recently, NaCl uptake across the apical membrane has been proposed to be mediated by parallel Na/H-Cl/formate exchangers (7–10). Such a mechanism of NaCl uptake requires that formic acid recycle across the apical membrane at a rate equal to the rate of transcellular chloride absorption. Karniski and Aronson (7) demonstrated that formic acid could enter brush border membrane vesicles by nonionic diffusion, but did not measure the formic acid permeability.

The purpose of the present studies was to measure the H and formic acid permeabilities of the apical and basolateral membranes of the rat PCT perfused in vivo. Membrane permeabilities were measured by examining the effect on intracellular pH (pH_i) of an H or formic acid gradient. From these measurements, the contributions of cellular leak pathways to net $NaHCO_3$ and NaCl absorption are estimated.

Methods

Rats were prepared for in vivo microperfusion as described previously (11). Rats received an intravenous infusion at 1.5 cm^3/h of Ringers' bicarbonate containing (in millimolar): NaCl, 105; $NaHCO_3$, 25; Na_2HPO_4, 4; KCl, 5; $MgSO_4$, 1; and $CaCl_2$, 1.8. Capillary and luminal pipettes were placed as previously described (12, 13). Cells were loaded for 6 min with the acetoxymethyl derivative of (2',7')-bis-(carboxyethyl)-(5,6)-carboxyfluorescein (BCECF), and then studied using luminal and peritubular perfusion as previously described (12, 13). In our system luminal and peritubular fluid changes are 90% complete in < 1 s. The luminal and peritubular capillary perfusates are listed in Table I. All solutions were bubbled with 7% CO_2/93% O_2 at 37°C. The [calcium gluconate] was chosen to give a measured ionized $[Ca^{2+}]$ of 1.5–1.8 mM. Solution chemicals were purchased from Sigma Chemical Co. (St. Louis, MO).

Analysis and calculations

Measurement of pH_i. As described previously (12), fluorescence was measured alternately at 500- and 450-nm excitation (emission 530 nm) using an epifluorescence microscope with interference filters. All results were corrected for background. An excitation ratio (F_{500}/F_{450}) was then calculated and the results of our previous intracellular dye calibration (14) used to convert fluorescent excitation ratios to an apparent pH_i.

Rate of change in pH_i. The initial rate of change in pH_i (dpH_i/dt) was calculated as described previously (12). Briefly, during a fluid change fluorescence was followed with 500-nm excitation (pH-sensitive wavelength) on a chart recorder. The slope of a line drawn tangent to the initial deflection defined the initial rate of change of 500-nm fluorescence $[d(F_{500})/dt]$. Fluorescence at 450-nm excitation was not measurably affected in vitro or in vivo by solution pH or pH_i, respectively, and thus can be considered constant (reference 12, present studies). The initial rate of change in the fluorescent excitation ratio $[d(F_{500}/F_{450})/dt]$ was therefore calculated using the equation:

$$d(F_{500}/F_{450})dt = [d(F_{500})/dt]/F_{450}, \quad (1)$$

where F_{450} represents the 450-nm excitation fluorescence corrected for

Address correspondence to Dr. Patricia Preisig, Department of Internal Medicine, University of Texas Southwestern Medical Center, 5323 Harry Hines Blvd., Dallas, TX 75235-9030.

Received for publication 30 June 1988 and in revised form 19 January 1989.

1. *Abbreviations used in this paper:* BCECF, (2',7')-bis-(carboxyethyl)-(5,6)-carboxyfluorescein; PCT, proximal convoluted tubule; pH_i, intracellular pH.

J. Clin. Invest.

0021-9738/89/06/1859/09 $2.00
Volume 83, June 1989, 1859–1867

Table I. Solutions

	1	2	3	4	5	6	7
				mM			
MES	5	5	5	5	5	5	5
Hepes	25	25	25	25	25	25	25
Choline HCO_3	25	25	5	5	—	—	10
K gluconate	5	5	5	5	5	5	5
$MgSO_4$	1	1	1	1	1	1	1
Ca gluconate	3.6	3.6	3.6	3.6	3.6	3.6	3.6
NH_4HCO_3	—	—	—	—	—	—	15
Total formate	—	20	—	20	—	20	—
pH	7.31	7.31	6.62	6.62	5.50	5.50	7.31

All solutions were titrated with *N*-methyl-D-glucamine hydroxide at 37°C, brought to final osmolality of 295–300 mosM with sucrose, and bubbled with 7% CO_2/93% O_2 at 37°C.

background at the time of the fluid change (interpolated from the measurements before and after the fluid change). This initial rate of change in the fluorescence ratio was converted to an initial rate of change in pH_i (dpH_i/dt) by dividing by the slope of the in vivo calibration of BCECF [$d(F_{500}/F_{450})/dpH$].

Measurement of membrane H permeability. In these studies, the initial rate of change in pH_i was followed in response to a sudden change in luminal or peritubular fluid pH. In theory, such a change may lead to alterations in the fluxes of H, OH, or HCO_3. To minimize the contribution of HCO_3 movement to these fluxes, Na and Cl were totally removed from the solutions. While we cannot completely eliminate the possibility of OH or HCO_3 fluxes, we have chosen to analyze the data using the formalism of an apparent H permeability (assuming that H is the only species diffusing across the membrane). The membrane permeability to H (P_H nanoliters/millimeter per minute) was calculated from the equation:

$$P_H = \frac{\phi_H}{\Delta[H]}, \tag{2}$$

where ϕ_H is the initial rate of change in H flux, picomoles/millimeter per minute, and $\Delta[H]$ is the change in [H] achieved with the fluid change, millimoles/liter or equivalently picomoles/nanoliter. Cell voltage was not included in the driving force term because changes in luminal pH (15) and changes in peritubular pH in the absence of sodium (16) do not affect cell voltage. ϕ_H was calculated from the equation:

$$\phi_H = (dpH_i/dt)_H \cdot \beta \cdot \frac{V}{mm}, \tag{3}$$

where $(dpH_i/dt)_H$ is the initial rate of change in pH_i in response to a perfusate pH change, pH units/minute, calculated as described above; β is the buffer capacity, millimoles/liter · pH unit, measured as described below; and V/mm is the cellular volume per millimeter tubule length, liters/millimeter. Cellular volume was calculated assuming an inner radius of 15 μm and an outer radius of 25 μm.

Calculation of membrane formic acid permeability. In these experiments the rate of change in pH_i was followed in response to the sudden addition of formic acid/formate to the luminal or peritubular fluid. The membrane permeability to formic acid (HF) (P_{HF} nanoliters/millimeter per minute) was calculated from the equation:

$$P_{HF} = \frac{\phi_{HF}}{\Delta[HF]}, \tag{4}$$

where ϕ_{HF} is the initial rate of change in formic acid flux, picomoles/millimeter per minute, and $\Delta[HF]$ is the change in formic acid concentration achieved with the fluid change, millimoles/liter or equivalently picomoles/nanoliter. [HF] was calculated using a pK for formic acid at 37°C of 3.76.[2]

For some experiments the lumen and capillaries were initially perfused with a pH 7.31 solution (Table I, solution 1) in the absence of formic acid. Then the solution was rapidly changed to one of pH 5.50 containing 20 mM total formate ([formic acid] = 0.36 mM; Table I, solution 6). Since the fluid change involved both a change in [H] and [formic acid], the resultant dpH_i/dt reflected a change in both the flux of H and formic acid, ϕ_{Total}, picomoles/millimeter per minute. Therefore, ϕ_{HF} was calculated from the equation:

$$\phi_{HF} = \phi_{Total} - \phi_H, \tag{5}$$

where ϕ_H was determined from experiments in which the same pH change was made in the absence of formic acid. ϕ_{Total} was calculated from the equation:

$$\phi_{Total} = (dpH_i/dt)_{Total} \cdot \beta \cdot \frac{V}{mm}, \tag{6}$$

where $(dpH_i/dt)_{Total}$ is the initial rate of change in pH_i in response to perfusate pH and [formic acid] changes, pH units/minute, and β and V/mm are as described for Eq. 3. In other experiments formic acid permeability was measured without simultaneously making a pH change. For these experiments $\phi_{Total} = \phi_{HF}$, and thus Eq. 6 could be used directly to calculate ϕ_{HF}.

Intracellular buffer capacity. The intracellular buffer capacity was determined using the technique of NH_3/NH_4^+ addition as described previously (14, 17). The buffer capacity (β millimoles/liter · pH unit) was given by the formula:

$$\beta = [NH_4^+]_i/\Delta pH_i, \tag{7}$$

where $[NH_4^+]_i$ is the intracellular $[NH_4^+]$ after addition of NH_3/NH_4^+, and ΔpH_i is the change in pH_i on addition of NH_3/NH_4^+. The initial pH_i was calculated from the fluorescence excitation ratio just before the addition of NH_3/NH_4^+, and the final pH_i from the fluorescence ratio at the peak of the spike. The intracellular concentration of NH_4^+ was calculated as:

$$[NH_4^+]_i = [NH_4^+]_0 \cdot 10^{(pH_0 - pH_i)}, \tag{8}$$

where $[NH_4^+]_0$ is the $[NH_4^+]$ of the perfusate and pH_0 is the pH of the perfusate. pH_i was calculated from the fluorescence excitation ratio just after addition of NH_3/NH_4^+ (at the peak of the spike).

All results are expressed as mean±SE. Statistical significance was assessed by t test for paired or unpaired data as appropriate. Apical membrane permeabilities measured in nanoliters/millimeter per minute were converted to centimeters/second by treating the surface area as a smooth cylinder of 15-μm radius (luminal radius). To express this permeability per membrane surface area, these values were divided by 36 to account for the surface area of the brush border microvilli (18). Because the actual membrane surface areas are similar for apical and basolateral membranes (18), similar surface area corrections were used for basolateral membrane permeabilities.

2. The ionic strength of solutions 1–7 ranged from 0.058 to 0.099 M, values lower than the ionic strength of serum (0.156 M) or an ultrafiltrate-like solution (0.148 M). We were unable to find data on the relationship between ionic strength and pK for formic acid, but did find data for acetic acid (47), and assumed the two acids behaved similarly. Over the ionic strength range of 0.0418–0.1610 M, the pK for acetic acid increased from 4.7587 to 4.7635 (47). To two decimal points these values are not different; thus, we did not adjust the pK of formic acid for ionic strength in our calculations.

Results

Membrane permeability to protons

In the first series of studies the H permeabilities of the apical and basolateral membranes were measured by examining the rate of change in pH_i in response to a change in [H] of the luminal or peritubular fluid, respectively. As in all of the permeability studies described below, Na and Cl were completely removed from luminal and peritubular perfusates to prevent contributions from transporters coupled to these ions. In this series both the lumen and capillaries were initially perfused with an Na- and Cl-free solution of pH 7.31 (Table I, solution 1). When luminal perfusate pH was rapidly changed to 5.50 (Table I, solution 5), pH_i decreased from 7.58±0.08 to 7.39±0.10. A typical tracing is shown in Fig. 1. In six tubules the initial rate of change of pH_i was 1.14±0.14 pH units/min (dpH_i/dt; Table II). A similar pH change in the capillary perfusate caused pH_i to decrease from 7.46±0.13 to 7.29±0.16 at an initial rate of 1.46±0.40 pH units/min ($n = 6$; Table II). The alkaline pH_i observed before luminal or peritubular fluid acidification agrees with previous findings by us in tubules perfused in the absence of Na, and is due to inhibition of base exit (12).

To convert these initial rates of change in pH_i to an initial rate of change in H-equivalent flux across the membrane, the buffer capacity (β) of the cell was measured using the technique of NH_3/NH_4^+ addition as described previously (14, 17). In these studies initially both the lumen and capillaries were perfused with solution 1 (Table I). The capillary fluid was then rapidly changed to one that was similar except that 15 mM NH_4^+ was substituted for 15 mM choline (Table I, solution 7). As described in Methods, buffer capacity was calculated from the initial pH_i change. In seven tubules β = 64±12 mmol/liter · pH unit. This value is similar to the value previously reported by us in the presence of Na and Cl of 75 mmol/liter · pH unit (14). The present lower, though not statistically different, value reported in this series may be attributable to the lack of contribution of Na- and Cl-coupled transporters in this series.

Eq. 3 was then used to calculate the initial rate of change in H flux represented by the dpH_i/dt measurements. For the apical membrane this initial flux was 92±12 pmol/mm · min (Table II). Using a Δ[H] of 3.113×10^{-3} mM (pH of 5.50 vs. 7.31), the apical membrane H permeability was 2.94±0.37 $\times 10^4$ nl/mm · min (0.52±0.07 cm/s). The same set of calculations for the basolateral membrane yielded an initial rate of change in H flux of 118±32 pmol/mm · min and an H permeability of 3.79±1.04 $\times 10^4$ nl/mm · min (0.67±0.18 cm/s)[3] (Table II). Interestingly, the apical and basolateral membrane H permeabilities were similar.

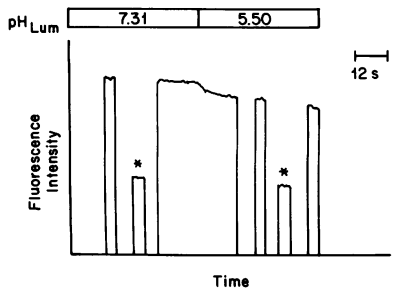

Figure 1. Typical tracings: time course of fluorescence intensity after a rapid change in luminal perfusate pH. Fluorescence intensity in arbitrary units is plotted on the *y* axis; time is on the *x* axis. Measurements taken with 450 nm excitation (the pH-insensitive wavelength) are denoted by the asterisks above the bars. All other measurements are taken with 500 nm excitation (pH-sensitive wavelength). During the fluid change from pH 7.31 to 5.50 (solution 1–5) 500 nm fluorescence is followed.

Membrane permeability to formic acid

Formic acid permeability measured at pH 5.50. In the next series of studies the formic acid permeability of the apical and basolateral membranes was measured. For these studies both the lumen and capillaries were initially perfused with solution 1 (Table I), and then changed to solution 6 (pH 5.50 plus 20 mM total formate; Table I) in either the lumen or capillary compartments. Fig. 2 (*left*) shows a typical tracing. When the luminal perfusate was rapidly changed, pH_i decreased from 7.44±0.08 to 6.73±0.06 at an initial rate of 3.60±0.48 pH units/min (Table III). Using Eq. 6 the initial rate of change in H and formic acid flux (ϕ_{Total}) was 289±38 pmol/mm · min. Using Eq. 5 this value was corrected for the H flux associated with the pH change (92 pmol/mm · min; Table II). The resultant initial rate of change in formic acid flux, ϕ_{HF}, was 197±38 pmol/mm · min. Using a Δ[HF] of 0.36 mM, Eq. 4 yielded an apical membrane formic acid permeability of 548±106 nl/mm · min ($1.0\pm0.2 \times 10^{-2}$ cm/s; Table III).

When the same fluid change was made in the capillary perfusate, pH_i decreased from 7.26±0.11 to 6.61±0.03 at an initial rate of 3.52±0.12 pH units/min ($n = 7$; Table III). This yielded a basolateral membrane formic acid permeability of 458±26 nl/mm · min ($0.8\pm0.1 \times 10^{-2}$ cm/s) (Table III). Once again the apical and basolateral membrane permeability values were very similar.

Response to symmetrical formate addition. As will be discussed later, the measured formic acid permeability is not sufficiently large to explain all of transcellular NaCl absorption. One concern in these studies was that the measured formic acid permeabilities were being significantly underestimated by the rapid flux of formic acid across the epithelium into the opposite fluid compartment which was serving as a "sink." To address this issue we performed studies as described above, except that simultaneous luminal and capillary fluid changes were made. We reasoned that if our measurements of formic acid permeability were correct, the flux measured with simultaneous fluid changes should approximately equal the sum of the fluxes of each of the membranes. On the other hand, if there was significant formic acid efflux from the cell to the opposite fluid compartment in the above studies, simultaneous fluid changes should lead to a flux far greater than the sum of the apparent fluxes of the two membranes. For these studies, in the control condition both the lumen and capillaries were perfused with solution 1 (Table I). The luminal and capillary fluids were then simultaneously changed to a pH 5.50 solution containing 20 mM total formate (Table I, solution 6). In response to these changes, pH_i rapidly acidified from 7.67±0.07 to 6.50±0.04 at an initial rate of 6.01±0.85 pH units/min, yielding a ϕ_{Total} of 483±68 pmol/mm · min ($n = 7$). This value was similar to the sum of the fluxes measured for the individual membranes (483 vs. 572 pmol/mm · min, re-

3. These permeabilities were measured at an extracellular pH of 5.50. While we acknowledge that exposure to this extracellular pH is unphysiologic, we were unable to make smaller pH changes and accurately measure dpH_i/dt because of the small change in driving force with smaller pH changes.

Table II. Apical and Basolateral Membrane Proton Permeabilities

	dpH_i/dt	H^+ flux	$\Delta([H^+]_o - [H^+]_i)$	P_H	P_H
	pH units/min	*pmol/mm · min*	*pmol/nl*	*×10⁴ nl/mm · min*	*cm/s*
Apical membrane	1.14±0.14	92±12	3.113×10^{-3}	2.94±0.37	0.52±0.07
Basolateral membrane	1.46±0.40	118±32	3.113×10^{-3}	3.79±1.04	0.67±0.18

spectively), demonstrating that the individual membrane measurements were not being significantly underestimated by a flux of formic acid across the epithelium into the opposite fluid compartment.

Formic acid permeability measured at pH 6.62. A second possible concern in the above measurements was that formic acid permeability was being measured at the nonphysiologic extracellular pH of 5.50. Therefore, we repeated this measurement at extracellular pH 6.62. A pH of 6.62 approximates the luminal pH where carbonic anhydrase–independent HCO_3 absorption and NaCl absorption occur (see Discussion). Also, so that no correction for effects of a pH change was required, pH was similar in control and experimental periods. A typical tracing is shown in Fig. 2 (*right*).

Lumen and capillaries were initially perfused with a solution of pH 6.62 (Table I, solution 3). When the luminal fluid was rapidly changed to one containing 20 mM total formate at pH 6.62 (Table I, solution 4), pH_i decreased from 6.78±0.05 to 6.65±0.05 at an initial rate of 0.95±0.13 pH units/min, yielding an apical membrane formic acid permeability of 2,716±374 nl/mm · min ($4.8 \pm 0.7 \times 10^{-2}$ cm/s, $n = 8$; Table III). When the same fluid change was made in the capillaries, pH_i decreased from 6.91±0.08 to 6.66±0.05 at an initial rate of 1.35±0.30 pH units/min, giving a basolateral membrane formic acid permeability of 3,861±859 nl/mm · min ($6.8 \pm 1.5 \times 10^{-2}$ cm/s, $n = 8$; Table III). Again, the formic acid permeabilities of the apical and basolateral membranes were similar.

In the above series both the luminal and peritubular fluids were pH 6.62. Whereas this pH represents the physiologic luminal fluid pH in the late proximal tubule, it is lower than the physiologic peritubular fluid pH. To rule out an effect of the lower peritubular pH on apical membrane formic acid permeability, an additional series was done. For these studies the capillaries were continuously perfused with a solution of pH 7.31 (Table I, solution 1). The lumen was initially perfused with a solution of pH 6.62 (Table I, solution 3), which was rapidly changed to one of similar pH but containing 20 mM total formate (Table I, solution 4). With this fluid change pH_i decreased from 7.04±0.08 to 6.89±0.08 at an initial rate of 0.84±0.15 pH units/min, yielding an apical membrane formic acid permeability of 2,402±419 nl/mm · min ($4.3 \pm 0.7 \times 10^{-2}$ cm/s, n = 5; Table III). This value is not statistically different from $4.8 \pm 0.7 \times 10^{-2}$ cm/s, measured at capillary pH 6.62 (see above), and therefore the two series were combined ($4.6 \pm 0.5 \times 10^{-2}$ cm/s).

Estimated basic formate flux. A third possible cause for underestimation of the measured formic acid permeabilities of the individual membranes was that basic formate was rapidly moving across the membrane, causing a cell alkalinization and blunting the cell acidification due to formic acid entry. To address this issue studies were performed to measure formate flux across the individual membranes. Initially both the lumen and capillaries were perfused with solution 1 (pH 7.31, Table I). Then, in either the lumen or capillaries, the fluid was rapidly changed to one of similar pH but containing 20 mM total formate (Table I, solution 2). In this solution, with 20 mM total formate at a pH of 7.31, the [formic acid] is only 0.006 mM; thus, formic acid flux should be negligible. When either a luminal or capillary fluid change was made, no transient deflection in the pH-sensitive, 500-nm excitation fluorescence intensity was observed, suggesting that there was not a rapid flux of formate into the cell. Steady-state pH_i decreased by 0.02±0.02 pH units with the luminal fluid change ($n = 8$), and by 0.05±0.03 pH units with the capillary fluid change ($n = 8$; NS vs. zero in both cases). Thus, even in a setting where no significant formic acid–induced acidification is expected, we did not find a significant formate-induced alkalinization. Therefore, the measurements of formic acid permeability were not underestimated by the concurrent movement of formate into the cell.

Discussion

The present studies measured the passive permeabilities of the apical and basolateral membranes of the rat proximal tubule

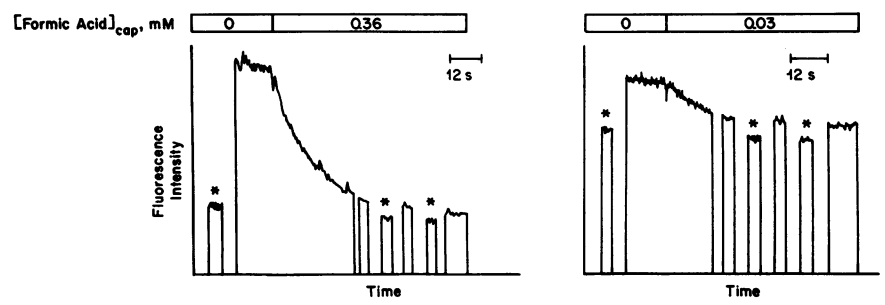

Figure 2. Typical tracings: time course of fluorescence intensity after a rapid change in peritubular [formic acid]±[H]. Fluorescence intensity in arbituary units is plotted on the *y* axis; time is on the *x* axis. Measurements taken with 450 nm excitation (pH-insensitive wavelength) are denoted by the asterisks above the bars. All other measurements are taken with 500 nm excitation (pH-sensitive wavelength). *Left,* fluorescence intensity after a change from solution 1 to solution 6 (pH 7.31 to pH 5.50 plus formic acid). *Right,* fluorescence intensity after a change from solution 3 to solution 4 (pH 6.62 to pH 6.62 plus formic acid).

Table III. Apical and Basolateral Membrane Formic Acid Permeabilities

	dpH_i/dt	Formic acid flux	Δ[HF]	P_{HF}	P_{HF}
	pH units/min	*pmol/mm · min*	*pmol/nl*	*nl/mm · min*	*$\times 10^{-2}$ cm/s*
Apical membrane					
Lumen perfusate, pH 7.31 → 5.50 + HF Capillary perfusate, pH 7.31	3.60±0.48	197±38	0.36	548±106	1.0±0.2
Lumen perfusate, pH 6.62±HF Capillary perfusate, pH 6.62	0.95±0.13	76±11	0.028	2,716±374	4.8±0.7
Lumen perfusate, pH 6.62±HF Capillary perfusate, pH 7.31	0.84±0.15	67±12	0.028	2,402±419	4.3±0.7
Basolateral membrane					
Lumen perfusate, pH 7.31 Capillary perfusate, pH 7.31 → 5.50 + HF	3.52±0.12	165±10	0.36	458±26	0.8±0.1
Lumen perfusate, pH 6.62 Capillary perfusate, pH 6.62±HF	1.35±0.30	108 ± 24	0.028	3,861±859	6.8±1.5

to H and formic acid. Na and Cl were removed from all solutions so that transporters coupled to these solutes would not contribute to the pH_i changes.

Role of the H leak. The apical and basolateral membrane H permeabilities were 0.52 and 0.67 cm/s, respectively. From these values a transcellular H permeability can be calculated using the following equation, which treats the two membranes as resistors in series:

$$\frac{1}{P_H^{\text{transcellular}}} = \frac{1}{P_H^{\text{apical}}} + \frac{1}{P_H^{\text{basolateral}}}.$$

This value, 0.29 cm/s, is very similar to the transepithelial values measured by Hamm et al. (19) and Schwartz (20), suggesting that the transcellular pathway plays a major role in passive transepithelial H fluxes.

Ives (21) measured an H permeability in brush border membrane vesicles, which when corrected for vesicle surface area and volume, and for brush border membrane amplification (multiplied by 36), was 0.47 cm/s, in agreement with our measured apical H permeability (0.52 cm/s). In pure lipid bilayers, Gutknecht (22) estimated H/OH permeabilities to be 1.4–5.8 $\times$ 10^{-4} cm/s at 24°C (using the same surface area correction for the brush border microvilli). These values are ~ 1/1,000 that measured or estimated for proximal tubule membranes (references 19–21, present studies). The lower permeability in lipid bilayers probably is due to the absence of membrane proteins that increase the hydrophilic nature of the epithelial membrane.

The contribution of an H leak to net $NaHCO_3$ absorption can be quantitated using our measured H permeabilities. The calculation for the early proximal tubule refers to a theoretical segment immediately after Bowman's space where the luminal fluid is an ultrafiltrate of plasma with $[HCO_3]$ = 25 mM. In this segment the calculated H leak from luminal fluid to cell is only 3 pmol/mm · min, an insignificant rate (see Appendix, part *a*). However, in the late proximal tubule where the luminal pH is more acidic, the net rate of transcellular H secretion is 42 pmol/mm · min (23), and the calculated H leak (lumen to cell) is 17 pmol/mm · min (see Appendix, part *a*). Therefore, the rate of active H secretion is actually 59 pmol/mm · min, with 33% of the flux leaking back into the cell. Thus, while the apical membrane H leak contributes little in the early proximal tubule, it may contribute significantly to end proximal net H secretion.

Across the basolateral membrane in both the early and late proximal tubule the rate of H leak from the peritubular fluid to cell is ~ 4 pmol/mm · min (see Appendix, part *a*). This flux contributes to net transepithelial HCO_3 absorption but is small in magnitude.

Formic acid permeability. In these studies, formic acid permeability was measured from the initial rate of change in pH_i in response to formic acid addition to either the luminal or peritubular fluid. Because of the low pK of formic acid and the high pH_i (relative to the pK), > 99.9% of formic acid entering the cell will immediately release its H, yielding formate. From the initial rate of change in pH_i and the cell's buffer capacity, we calculated the flux of formic acid into the cell, and using the chemical driving force, a formic acid permeability. In control studies we demonstrated that formic acid permeability was not underestimated by formic acid efflux from the cell on the opposite side. In addition, we demonstrated that in the absence of Na and Cl, basic formate does not enter the cell, and therefore does not affect these measurements. Formic acid permeability measured at pH 5.50 was 1.0 $\times$ 10^{-2} cm/s for the apical membrane and 0.8 $\times$ 10^{-2} cm/s for the basolateral membrane. Formic acid permeability measured at the more physiologic extracellular fluid pH of 6.62 was 4.6 $\times$ 10^{-2} cm/s for the apical membrane and 6.8 $\times$ 10^{-2} cm/s for the basolateral membrane. The reason for this apparent pH dependence of formic acid permeability is not presently clear. One possibility is that the pH 5.50 plus formic acid solution is more toxic to the cells than the pH 6.62 plus formic acid solution. While we do not believe that there is cell toxicity in any of the series, we cannot rule it out. A second possibility is that the buffer capacity used to calculate the formic acid flux must be adjusted for the baseline pH_i in the two series. The effect of using a unique buffer capacity is quantitated in part *b* of the Appendix. As can be seen, this correction can account for some but not all of the discrepancy. A third possibility is that the difference is secondary to pH effects on the packing of lipids in the lipid bilayer. Diamond and Wright (24) have noted that nonelectrolyte permeabilities can be pH dependent, with lower permeabilities associated with more acidic pHs. In any case, it is not the purpose of these studies to examine the pH dependence of the

permeability; the permeability measured at pH 6.62 is clearly the more physiologically relevant value.

In the rabbit proximal tubule Schild et al. (personal communication), measuring the effect of luminal formate addition on cell volume, estimated an apical membrane formic acid permeability of 36×10^{-2} cm/s (normalized for cylindrical surface area). This value is eight times larger than that measured in the present studies. Walter and Gutknecht (25) found that formic acid permeability in egg phosphatidylcholine-decane and bacterial phosphatidyl ethanolamine-squalene lipid bilayers ranged from 0.004 to 0.01 cm/s. Assuming that brush border microvilli increase the apical surface area 36-fold (18), this would be equivalent to an apical membrane permeability of $14–36 \times 10^{-2}$ cm/s (normalized for cylindrical surface area).

In comparing nonelectrolyte permeabilities in lipid bilayers with those in biological membranes, the effect of cholesterol content of the membrane must be considered. Finkelstein has demonstrated that the addition of cholesterol reduces the bilayer permeability to nonelectrolytes (26). Formic acid permeability measured in red blood cells (RBC) (~ 1:1 ratio phospholipid/cholesterol) is approximately fivefold smaller than formic acid permeability measured in egg phosphatidylcholine-decane and bacterial phosphatidylethanolamine-squalene lipid bilayers (25). Brush border membranes also have a ~ 1:1 ratio of phospholipid/cholesterol (27), and our measured formic acid permeability is 2–6 times smaller than that in cholesterol-free phospholipid bilayers, and very similar to that in red blood cells (4.6×10^{-2} cm/s vs. 5.5×10^{-2} cm/s [28] [normalized for cylindrical area], respectively).

Formic acid recycling across the apical membrane in NaCl absorption. Apical membrane NaCl uptake is inhibited by luminal amiloride and disulfonic stilbenes (29–31), implying that it is mediated by Na/H exchange operating in parallel with Cl/base exchange. While vesicle studies have found apical membrane Cl/OH exchange (1), Karniski and Aronson (7) found much faster rates of Cl/formate exchange. Studies in intact tubules have confirmed the presence of formate-independent and -dependent Cl/base exchange, with the formate-dependent transporter being faster (9, 10). Schild et al. (8) found that addition of small concentrations of formate to luminal and peritubular fluids of the proximal tubule stimulated volume (and presumably NaCl) absorption. These results are all consistent with apical membrane NaCl uptake mediated by Na/H exchange in parallel with Cl/OH and Cl/formate exchange. In order for parallel Na/H and Cl/formate exchange to mediate NaCl uptake across the apical membrane, formic acid must recycle across the apical membrane at a rate equal to the rate of this mode of transcellular NaCl absorption. Alpern et al. (3) demonstrated that the rate of transcellular NaCl absorption in the rat PCT was ~ 100–130 pmol/mm · min. In these studies, while solvent drag could not explain the entire transcellular flux, it could have contributed and led to somewhat of an overestimate of the transcellular flux.

The rate of formic acid movement across the apical membrane can be calculated from the equation $\phi_{HF}^{apical} = P_{HF}^{apical} \cdot ([HF]_{lumen} - [HF]_{cell})$, where ϕ_{HF}^{apical} is the formic acid flux across the apical membrane, picomoles/millimeter per minute, P_{HF}^{apical} is the apical membrane formic acid permeability, nanoliters/millimeter per minute, and $([HF]_{lumen} - [HF]_{cell})$ is the driving force for formic acid diffusion in millimolar. Using this equation with overestimates for the driving force, the calculated rate of formic acid diffusion is 4.7 pmol/mm · min (see Appendix, part *c*), < 5% of the measured rate of transcellular NaCl absorption (100–130 pmol/mm · min [3]). Schild et al. (8) demonstrated that formate addition to the perfusates in the in vitro perfused rabbit proximal tubule doubled the rate of volume absorption associated with active NaCl absorption, suggesting that Cl/formate exchange mediated ~ 50% of transcellular NaCl absorption. The present studies suggest that the rate of formic acid recycling limits the contribution of Cl/formate exchange to a smaller percentage in the rat.

One possible explanation for higher than calculated rates of formic acid recycling is a luminal unstirred layer. If such an unstirred layer was present, parallel apical membrane Na/H and Cl/formate exchangers would establish a high local total formate concentration and a low local pH. However, the unstirred layer would need to create at least an eightfold increase in the driving force for formic acid recycling to account for 50% of the measured rate of transcellular NaCl absorption.

In addition to Cl/formate exchange with formic acid recycling, a significant fraction of NaCl absorption may be mediated by Cl/OH exchange with H_2O recycling. While rates of Cl/formate exchange exceed rates of Cl/OH exchange in vesicle and tubule studies (7, 9, 10), the abundance of H_2O compared with formic acid may allow the Cl/OH exchanger to play a greater role in NaCl absorption. Indeed, in the studies of Schild et al. (8), ~ 50% of transcellular NaCl absorption remained in the absence of formate. Other possible mechanisms for NaCl uptake, which would not require formic acid recycling, include Na/formate cotransport operating in parallel with Cl/formate exchange. While formate does not compete with lactate on the Na/lactate cotransporter (32), the existence of a separate Na/formate transporter has not been ruled out. Another possible mechanism is Na/H exchange operating in parallel with Cl/oxalate exchange with oxalic acid recycling. There is evidence for Cl/oxalate exchange in brush border membrane vesicle studies (33), but oxalic acid permeability and the contribution of this mechanism to NaCl absorption have not been quantitated.

Carbonic acid (H_2CO_3) recycling. Carbonic anhydrase, located on the apical membrane and in the cytoplasm, contributes to HCO_3 absorption by catalyzing the effective dehydration of luminal H_2CO_3 to CO_2, and rehydration of cellular CO_2 to H_2CO_3, thus ensuring that the secreted H is recycled. While inhibition of carbonic anhydrase significantly inhibits proximal tubular HCO_3 absorption, it is interesting to note that a significant flux of HCO_3 absorption persists. This small carbonic anhydrase–independent HCO_3 flux, 10–30 pmol/mm · min (34–39), is greater than can be explained by the uncatalyzed rates of luminal H_2CO_3 dehydration and cellular CO_2 hydration, making it unclear how the secreted H would recycle from lumen to cell for a continued supply of intracellular H. Rector et al. (40) proposed that H_2CO_3 itself could recycle across the apical membrane. Because CO_2 diffusion is rapid, it has been considered impossible to directly measure H_2CO_3 permeability.

If formic acid permeability is used as an estimate of carbonic acid permeability, the flux of carbonic acid across the apical membrane ($\phi_{H_2CO_3}^{apical}$ picomoles/millimeter per minute) would be given by the equation $\phi_{H_2CO_3}^{apical} = P_{H_2CO_3}^{apical} \cdot ([H_2CO_3]_{lumen} - [H_2CO_3]_{cell})$. As calculated in part *d* of the Appendix, this leads to an estimated rate of H_2CO_3 recycling of 18–42 pmol/mm · min, suggesting that carbonic acid recycling can explain a significant fraction of carbonic anhydrase–inde-

Table IV. Effect of Buffer Capacity on P_H and P_{HF}

	P_{H^+} apical	P_{H^+} basolateral	Transcellular P_{H^+} calculated	P_{HF} apical membrane: *L 7.31 → 5.50 + HF ‡C 7.31	P_{HF} apical membrane: L 6.62±HF C 6.62	P_{HF} apical membrane: L 6.62±HF C 7.31	P_{HF} basolateral membrane: L 7.31 C 7.31 → 5.50 + HF	P_{HF} basolateral membrane: L 6.62 C 6.62±HF
	cm/s	*cm/s*	*cm/s*	*×10⁻² cm/s*	*×10⁻² cm/s*	*×10⁻² cm/s*	*×10⁻² cm/s*	*×10⁻² cm/s*
$\beta_T = 64 \frac{mM}{pH\ unit}$	0.52	0.67	0.29	1.0	4.8	4.3	0.8	6.8
$\beta_T = 18 + \beta_{CO_2/HCO_3} \frac{mM}{pH\ unit}$	0.82	1.05	0.46	1.5	2.8	3.2	1.3	4.0

Comparison of calculated permeabilities using two estimates of β; one is constant, and one varies as a function of pH_i. * L, luminal perfusate pH. ‡ C, capillary perfusate pH.

pendent HCO_3 absorption. Unfortunately, this calculation assumes that carbonic acid (H_2CO_3) permeability is equal to formic acid (H_2CO_2) permeability, an unproven assumption.[4]

Appendix

(a) Calculation of apical and basolateral membrane H flux

The rate of H backleak (J_H) was calculated from the Goldman, Hodgkins, Katz equation (41), assuming cell $PD = -60$ mV:

$$J_H = \frac{P_H \frac{ZF}{RT}([H]_0 - [H]_i e^{\frac{-ZF}{RT}})}{1 - e^{\frac{-ZF}{RT}}}$$

where Z, F, R, and T are valence, Faraday constant, gas constant, and degrees Kelvin, respectively.

(*i*) *Apical membrane H backleak in the early proximal tubule.* This calculation refers to a theoretical early proximal tubule segment immediately after Bowman's space where the luminal fluid is an ultrafiltrate of plasma. For this calculation we used a luminal fluid pH of 7.32 ($[H]_0$ = 48 nmol/liter) corresponding to a $[HCO_3]$ = 25 mM and pCO_2 = 50 mmHg, and pH_i = 7.20 ($[H]_i$ = 63 nmol/liter). The calculated J_H is 3.1 pmol/mm · min, using the measured apical membrane P_H of 2.94 × 10^4 nl/mm · min.

(*ii*) *Apical membrane H backleak in the late proximal tubule.* For this calculation we used a luminal fluid pH of 6.62, corresponding to a luminal $[HCO_3]$ = 5 mM, to simulate late proximal tubule conditions, ($[H]_0$ = 238 nmol/liter), and pH_i = 7.20 ($[H]_i$ = 63 nmol/liter). The calculated J_H is 16.8 pmol/mm · min, using a P_H of 2.94 × 10^4 nl/mm · min.

(*iii*) *Basolateral membrane H backleak.* For this calculation we used a peritubular pH of 7.32 ($[H]_0$ = 48 nmol/liter) and pH_i = 7.20 ($[H]_i$ = 63 nmol/liter). The calculated J_H is 3.9 pmol/mm · min, using the measured basolateral membrane P_H of 3.79 × 10^4 nl/mm · min. If peritubular fluid pH is lower, pH 7.27, as measured in the stellate vessel (42), the rate of backleak would be increased to 4.5 pmol/mm · min.

(b) Effect of buffer capacity on H and formic acid permeabilities

Our buffer capacity (β_{Total}) of 64 mmol/liter · pH unit measured in the absence of Na and Cl was used in all studies to convert dpH_i/dt (pH units/minute) to an apparent H-equivalent flux. In these studies baseline pH_i varied depending on the pH of the luminal and capillary perfusates (pH_i 7.48 with pH 7.31/7.31 (luminal/peritubular) perfusates, pH_i 7.04 with pH 6.62/7.31 perfusates, and pH_i 6.85 with 6.62/6.62 perfusates). β_{Total} is equal to $\beta_{nonCO_2/HCO_3} + \beta_{CO_2/HCO_3}$. Whereas β_{nonCO_2/HCO_3} has been shown to vary as a function of pH_i in barnacle muscle fibers (43), it has been shown to be constant in proximal tubule cells over the pH range of 6.3–7.3 (44). In our studies β was measured at pH_i = 7.23. Under these conditions our calculated β_{nonCO_2/HCO_3} is 18 mmol/liter · pH unit, in close agreement with that measured in proximal tubule cells (44) of 24 mmol/liter · pH unit. However, it is likely that β_{CO_2/HCO_3} (equal to 2.3[HCO_3] [17]) varied in the different series of the present studies since baseline pH_i and cell $[HCO_3]$ varied. Table IV calculates P_H and P_{HF} for each series by using a β unique to pH_i. β_{Total} was calculated as $\beta_{Total} = \beta_{nonCO_2/HCO_3} + \beta_{CO_2/HCO_3}$, where β_{nonCO_2/HCO_3} = 18 mmol/liter · pH unit and $\beta_{CO_2/HCO_3} = 2.3[HCO_3]_i$.

(c) Rate of formic acid recycling across the apical membrane

The flux of formic acid across the apical membrane (ϕ_{HF}^{apical} picomoles/millimeter per minute) was calculated from the equation $\phi_{HF}^{apical} = P_{HF}^{apical} \cdot ([HF]_{lumen} - [HF]_{cell})$, where P_{HF}^{apical} is the measured apical membrane formic acid permeability (4.6 × 10^{-2} cm/s), and $[HF]_{lumen}$ and $[HF]_{cell}$ are the formic acid concentrations of the luminal fluid and cell, respectively. $[HF]_{lumen}$ was calculated from the equation:

$$[HF]_{lumen} = \frac{\text{Total [Formate]}_{lumen}}{1 + 10^{(pH_L - pK_{HF})}},$$

where total formate concentration was assumed to be 1 mM (7). We used a luminal fluid pH (pH_L) of 6.50 to simulate the pH of the luminal fluid in the late proximal tubule where the majority of NaCl absorption occurs. If the luminal pH in the late proximal tubule is > 6.50, $[HF]_{lumen}$ will decrease and ϕ_{HF}^{apical} will decrease.

For this calculation, $[HF]_{cell}$ was assumed to be zero, an underestimate which will lead to an overestimate of the flux. Using these values, ϕ_{HF}^{apical} = 4.7 pmol/mm · min. All of our assumptions tend to overestimate the rate of formic acid recycling across the apical membrane.

(d) Rate of carbonic acid recycling across the apical membrane

The rate of carbonic acid (H_2CO_3) recycling ($\phi_{H_2CO_3}^{apical}$ picomoles/millimeter per minute) was calculated from the equation $\phi_{H_2CO_3}^{apical} = P_{H_2CO_3}^{apical} \cdot ([H_2CO_3]_{lumen} - [H_2CO_3]_{cell})$, where $P_{H_2CO_3}^{apical}$ is the apical membrane permeability to carbonic acid, and $[H_2CO_3]_{lumen}$ and $[H_2CO_3]_{cell}$ are the [carbonic acid] of the luminal fluid and cell, respectively. As described in the text, it is not possible to measure $P_{H_2CO_3}^{apical}$ directly because the $[H_2CO_3]$ in a solution is $\ll [CO_2]$, and CO_2 is readily permeable across lipid bilayers. Therefore, we used our formic acid (H_2CO_2) permeability, 4.6 × 10^{-2} cm/s, to estimate carbonic acid

4. The issue of whether or not formic acid permeability is a good estimate of carbonic acid permeability is very complex. The difference between a formic acid and a carbonic acid molecule is the substitution of an OH group for an H on the formic acid molecule. The effect of this change on membrane permeability depends on the number and strength of the hydrogen bonds formed by the substituting OH group with the surrounding H_2O (24). The larger the number or stronger the bonds, the more the membrane permeability will be decreased (24).

(H_2CO_3) permeability, noting the concerns raised in footnote 4. $[H_2CO_3]_{lumen}$ and $[H_2CO_3]_{cell}$ were calculated from the equation:

$$[H_2CO_3]_x = \frac{[HCO_3]_x}{1 + 10^{(pH_x - pK_{H_2CO_3})}},$$

where the $pK_{H_2CO_3} = 3.57$, and $[HCO_3]_x$, pH_x, and $[H_2CO_3]_x$ are the $[HCO_3]$, pH, and [carbonic acid] of either the luminal fluid or cell. $[H_2CO_3]_{lumen}$ was calculated as the mean luminal concentration using a mean luminal pH in the presence of carbonic anhydrase inhibitors of 6.7–7.0 (42, 45, 46), and a mean luminal $[HCO_3]$ in the presence of carbonic anhydrase inhibitors of 25 mM (equal to ultrafiltrate $[HCO_3]$). This value was chosen because Lucci et al. (37) and Cogan et al. (38) demonstrated that luminal $[tCO_2]$ does not decrease below plasma levels in the presence of carbonic anhydrase inhibitors. To calculate $[H_2CO_3]_{cell}$, $pH_i = 7.4$ was chosen because we have shown that when acetazolamide was added to the peritubular perfusate, pH_i increased from ~ 7.2 to 7.4 (unpublished observations). We used a cell $[HCO_3]$ of 15 mM. These values give a range for $[H_2CO_3]_{lumen}$ of 9.3–18.5 μM and a $[H_2CO_3]_{cell}$ of 2.2 μM. Using the formic acid permeability of the apical membrane for P_{H2CO3}^{apical}, an estimate of ϕ_{H2CO3}^{apical} is 18–42 pmol/mm · min.

Acknowledgments

The authors would like to thank John Gutknecht for his helpful discussions on formic acid permeability, and Ms. Linda Poellnitz for her excellent secretarial assistance.

This work was supported by National Institutes of Diabetes, Digestive, and Kidney Disease grant R01-DK39298, Biomedical Research Support grant 2-507-RR05426-26, a grant from the National Kidney Foundation of Texas, and funds from the Ruby B. Hexter estate.

References

1. Alpern, R. J. 1988. Cell mechanisms of proximal tubule acidification. *Physiol. Rev.* In press.

2. Howlin, K. J., R. J. Alpern, C. A. Berry, and F. C. Rector, Jr. 1986. Evidence for electroneutral sodium chloride transport in rat proximal convoluted tubule. *Am. J. Physiol.* 250 (*Renal Fluid Electrolyte Physiol.* 19):F644–F648.

3. Alpern, R. J., K. J. Howlin, and P. A. Preisig. 1985. Active and passive components of chloride transport in the rat proximal convoluted tubule. *J. Clin. Invest.* 76:1360–1366.

4. Chantrelle, B. M., M. G. Cogan, and F. C. Rector, Jr. 1985. Active and passive components of NaCl absorption in the proximal convoluted tubule of the rat kidney. *Miner. Electrolyte Metab.* 11:209–214.

5. Baum, M., and C. A. Berry. 1984. Evidence for neutral transcellular NaCl transport and neutral basolateral chloride exit in the rabbit proximal convoluted tubule. *J. Clin. Invest.* 74:205–211.

6. Green, R., J. H. V. Bishop, and G. Giebisch. 1979. Ionic requirements of proximal tubular sodium transport. III. Selective luminal anion substitution. *Am. J. Physiol.* 236 (*Renal Fluid Electrolyte Physiol.* 5):F268–F277.

7. Karniski, L. P., and P. S. Aronson. 1985. Chloride/formate exchange with formic acid recycling: a mechanism of active chloride transport across epithelial membranes. *Proc. Natl. Acad. Sci. USA.* 82:6362–6365.

8. Schild, L., G. Giebisch, L. P. Karniski, and P. S. Aronson. 1987. Effect of formate on volume reabsorption in the rabbit proximal tubule. *J. Clin. Invest.* 79:32–38.

9. Alpern, R. J. 1987. Apical membrane chloride/base exchange in the rat proximal convoluted tubule. *J. Clin. Invest.* 79:1026–1030.

10. Baum, M. 1988. Effect of luminal chloride on cell pH in rabbit proximal tubule. *Am. J. Physiol.* 254 (*Renal Fluid Electrolyte Physiol.* 23):F677–F683.

11. Preisig, P. A., H. E. Ives, E. J. Cragoe, Jr., R. J. Alpern, and F. C. Rector, Jr. 1987. Role of the Na^+/H^+ antiporter in rat proximal tubule bicarbonate absorption. *J. Clin. Invest.* 80:970–978.

12. Alpern, R. J. 1985. Mechanism of basolateral membrane $H^+/OH^-/HCO_3^-$ transport in the rat proximal convoluted tubule. *J. Gen. Physiol.* 86:613–636.

13. Alpern, R. J., and M. Chambers. 1986. Cell pH in the rat proximal convoluted tubule: regulation by luminal and peritubular pH and sodium concentration. *J. Clin. Invest.* 78:502–510.

14. Preisig, P. A., and R. J. Alpern. 1988. Chronic metabolic acidosis causes an adaptation in the apical membrane Na/H antiporter and basolateral membrane $Na(HCO_3)_3$ symporter in the rat proximal convoluted tubule. *J. Clin. Invest.* 82:1445–1453.

15. Burckhardt, B.-Ch., K. Sato, and E. Fromter. 1984. Electrophysiological analysis of bicarbonate permeation across the peritubular cell membrane of rat kidney proximal tubule. I. Basic observations. *Pfluegers Arch. Eur. J. Physiol.* 401;34–43.

16. Yoshitomi, K., B.-Ch. Burckhardt, and E. Fromter. 1985. Rheogenic sodium-bicarbonate cotransport in the peritubular cell membrane of rat renal proximal tubule. *Pfluegers Arch. Eur. J. Physiol.* 405:360–366.

17. Roos, A., and W. F. Boron. 1981. Intracellular pH. *Physiol. Rev.* 61:297–434.

18. Welling, L. W., and D. J. Welling. 1975. Surface areas of brush border and lateral cell walls in the rabbit proximal nephron. *Kidney Int.* 8:343–348.

19. Hamm, L. L., L. R. Pucacco, J. P. Kokko, and H. R. Jacobson. 1984. Hydrogen ion permeability of the rabbit proximal convoluted tubule. *Am. J. Physiol.* 246 (*Renal Fluid Electrolyte Physiol.* 15):F3–F11.

20. Schwartz, G. J. 1981. Na^+-dependent H^+ efflux from proximal tubule: evidence for reversible Na^+-H^+ exchange. *Am. J. Physiol.* 241 (*Renal Fluid Electrolyte Physiol.* 10):F380–F385.

21. Ives, H. E. 1985. Proton/hydroxyl permeability of proximal tubule brush border vesicles. *Am. J. Physiol.* 248 (*Renal Fluid Electrolyte Physiol.* 17):F78–F86.

22. Gutknecht, J. 1987. Proton/hydroxide conductance and permeability through phospholipid bilayer membranes. *Proc. Natl. Acad. Sci. USA.* 84:6443–6446.

23. Alpern, R. J., M. G. Cogan, and F. C. Rector, Jr. 1982. Effect of luminal bicarbonate concentration on proximal acidification in the rat. *Am. J. Physiol.* 243 (*Renal Fluid Electrolyte Physiol.* 12):F53–F59.

24. Diamond, J. M., and E. M. Wright. 1969. Biological membranes: the physical basis of ion and nonelectrolyte selectivity. *Annu. Rev. Physiol.* 31:581–645.

25. Walter, A., and J. Gutknecht. 1984. Monocarboxylic acid permeation through lipid bilayer membranes. *J. Membr. Biol.* 77:255–264.

26. Finkelstein, A. 1976. Water and nonelectrolyte permeability of lipid bilayer membranes. *J. Gen. Physiol.* 68:127–135.

27. Molitoris, B. A., and F. R. Simon. 1985. Renal cortical brush-border and basolateral membranes: cholesterol and phospholipid composition and relative turnover. *J. Membr. Biol.* 83:207–215.

28. Klocke, R. A., K. K. Andersson, H. H. Rotman, and R. E. Forster. 1972. Permeability of human erythrocytes to ammonia and weak acids. *Am. J. Physiol.* 222(3):1004–1013.

29. Lucci, M. S., and D. G. Warnock. 1979. Effects of anion-transport inhibitors on NaCl reabsorption in the rat superficial proximal convoluted tubule. *J. Clin. Invest.* 64:570–579.

30. Baum, M. 1987. Evidence that parallel Na^+-H^+ and Cl^--$HCO_3^-(OH^-)$ antiporters transport NaCl in the proximal tubule. *Am. J. Physiol.* 252 (*Renal Fluid Electrolyte Physiol.* 21):F338–F345.

31. Preisig, P. A., and F. C. Rector, Jr. 1988. Role of the Na^+/H^+ antiporter in rat proximal tubule NaCl absorption. *Am. J. Physiol.* 255 (*Renal Fluid Electrolyte Physiol.* 24):F461–F465.

32. Nord, E. P., S. H. Wright, I. Kippen, and E. M. Wright. 1983. Specificity of the Na^+-dependent monocarboxylic acid transport pathway in rabbit renal brush border membranes. *J. Membr. Biol.* 72:213–221.

33. Karniski, L. P., and P. S. Aronson. 1987. Anion exchange pathways for Cl^- transport in rabbit renal microvillus membranes. *Am. J. Physiol.* 253 (*Renal Fluid Electrolyte Physiol.* 22):F513–F521.

34. Alpern, R. J. 1984. Bicarbonate-water interactions in the rat proximal convoluted tubule: an effect of volume flux on active proton secretion. *J. Gen. Physiol.* 84:753–770.

35. Cogan, M. G., and F. C. Rector, Jr. 1982. Determinants of proximal bicarbonate, chloride, and water reabsorption during carbonic anhydrase inhibition. *Am. J. Physiol.* 242 (*Renal Fluid Electrolyte Physiol.* 11):F274–F284.

36. Chan, Y. L., B. Biagi, and G. Giebisch. 1982. Control mechanisms of bicarbonate transport across the rat proximal convoluted tubule. *Am. J. Physiol.* 242 (*Renal Fluid Electrolyte Physiol.* 11):F532–F543.

37. Lucci, M. S., L. R. Pucacco, T. D. DuBose, Jr., J. P. Kokko, and N. W. Carter. 1980. Direct evaluation of acidification by rat proximal tubule: role of carbonic anhydrase. *Am. J. Physiol.* 238 (*Renal Fluid Electrolyte Physiol.* 7):F372–F379.

38. Cogan, M. G., D. A. Maddox, D. G. Warnock, E. T. Lin, and F. C. Rector, Jr. 1979. Effect of acetazolamide on bicarbonate reabsorption in the proximal tubule of the rat. *Am. J. Physiol.* 237(6):F447–F454.

39. Jacobson, H. R. 1981. Effects of CO_2 and acetazolamide on bicarbonate and fluid transport in rabbit proximal tubules. *Am. J. Physiol.* 240 (*Renal Fluid Electrolyte Physiol.* 9):F54–F62.

40. Rector, F. C., Jr., D. W. Seldin, A. D. Roberts, Jr., and J. S. Smith. 1960. The role of plasma CO_2 tension and carbonic anhydrase activity in the renal reabsorption of bicarbonate. *J. Clin. Invest.* 39:1706–1721.

41. Verkman, A. S., and R. J. Alpern. 1987. Kinetic transport model for cellular regulation of pH and solute concentration in the renal proximal tubule. *Biophys. J.* 51:533–546.

42. DuBose, T. D., Jr., L. R. Pucacco, M. S. Lucci, and N. W. Carter. 1979. Micropuncture determination of pH, PCO_2, and total CO_2 concentration in accessible structures of the rat renal cortex. *J. Clin. Invest.* 64:476–482.

43. Boron, W. F. 1977. Intracellular pH transients in giant barnacle muscle fibers. *Am. J. Physiol.* 233 (*Cell Physiol.* 2):C61–C73.

44. Bidet, M., M. Tauc, J. Merot, A. Vandewalle, and P. Poujeol. 1987. Na^+-H^+ exchanger in proximal cells isolated from rabbit kidney. I. Functional characteristics. *Am. J. Physiol.* 253 (*Renal Fluid Electrolyte Physiol.* 22):F935–F944.

45. Vieira, F. L., and G. Malnic. 1968. Hydrogen ion secretion by rat renal cortical tubules as studied by an antimony microelectrode. *Am. J. Physiol.* 214(4):710–718.

46. Rector, F. C., Jr., N. W. Carter and D. W. Seldin. 1965. The mechanism of bicarbonate reabsorption in the proximal and distal tubules of the kidney. *J. Clin. Invest.* 44:278–290.

47. MacInnes, D. A. 1961. The Principles of Electrochemistry. Dover Publications, New York. 202–212.